

RESEARCH ARTICLE

Open Access



Transcriptomic and lipidomic analysis of aging-associated inflammatory signature in mouse liver

Tomoaki Ishihara^{1,2*}, Hiroshi Tsugawa^{1,3,4,5}, Seigo Iwanami^{1,6}, Jen-Chien Chang⁷, Aki Minoda^{7,8} and Makoto Arita^{1,5,6*}

Abstract

Background Aging-associated dysbiosis leads to chronic inflammation and the development of a range of aging-related diseases. The gut microbiota crosstalks with the host by providing lipid metabolites and modulating metabolic functions. However, the precise mechanism by which the gut microbiota regulates aging is unknown. The objective of this study was to examine the impact of the gut microbiota on the transcriptome and lipidome associated with aging in mouse liver.

Methods RNA-sequencing was conducted on the livers of young and aged male and female-specific pathogen-free (SPF) and germ-free (GF) mice to comprehensively analyze transcriptomic alterations with aging. We also reanalyzed our previously reported results on aging-associated changes in the hepatic lipidome to investigate the gut microbiota-dependent hepatic lipidome signatures associated with aging.

Results In contrast to the findings in male mice, the changes in hepatic transcriptome associated with aging were attenuated in female GF mice compared with those in SPF mice. In particular, the gene sets associated with inflammatory signatures (i.e., inflammation and tissue remodeling) were found to be suppressed in female GF mice. The ChIP-Atlas database predicted that transcription factors associated with sex differences may be involved in the gene signature of aged female GF mice. Significant differences in the lipid profile were observed between aged SPF and GF female mice, including in bile acids, sterol sulfates, lysophospholipids, oxidized triacylglycerols, vitamin D, and phytoceramides. Moreover, notable alterations were identified in the quality of phospholipids and sphingolipids. Integrated transcriptomic and lipidomic analysis identified candidate enzymes responsible for the change of lipid profiles in aged female mice.

Conclusions The findings of this study offer new insights into the molecular mechanisms through which the gut microbiota regulates aging-related phenotypes such as inflammation in the liver, possibly through modulating lipid metabolism in a sex-dependent manner.

Keywords Aging, Gut microbiota, Inflammation, Lipid metabolism, Sex difference, Germ-free

*Correspondence:

Tomoaki Ishihara
tomoaki.ishihara@niu.ac.jp
Makoto Arita
makoto.arita@riken.jp

Full list of author information is available at the end of the article



© The Author(s) 2025. **Open Access** This article is licensed under a Creative Commons Attribution-NonCommercial-NoDerivatives 4.0 International License, which permits any non-commercial use, sharing, distribution and reproduction in any medium or format, as long as you give appropriate credit to the original author(s) and the source, provide a link to the Creative Commons licence, and indicate if you modified the licensed material. You do not have permission under this licence to share adapted material derived from this article or parts of it. The images or other third party material in this article are included in the article's Creative Commons licence, unless indicated otherwise in a credit line to the material. If material is not included in the article's Creative Commons licence and your intended use is not permitted by statutory regulation or exceeds the permitted use, you will need to obtain permission directly from the copyright holder. To view a copy of this licence, visit <http://creativecommons.org/licenses/by-nc-nd/4.0/>.

Background

Aging is a complex process characterized by progressive changes in the physiological functions of various organs. This in turn increases the risk of developing chronic inflammatory diseases including metabolic syndrome, metabolic dysfunction-associated fatty liver disease (MAFLD), neurodegenerative diseases, and cancer [1, 2]. Dysregulated composition of gut microbiota (dysbiosis), chronic low-grade inflammatory responses, and abnormal metabolic functions involving lipids are frequently associated with aging and are implicated in the development of aging-related diseases [3–7].

The gut microbiota plays an important role in maintaining host homeostasis, including digestion and absorption of food, production of nutrients, and regulation of the host immune system [8, 9]. Changes in the composition of the gut microbiota associated with aging have implications for human health and longevity [1, 10]. Meanwhile, in mice, fecal transplantation from aged specific pathogen-free (SPF) mice into young germ-free (GF) mice has been shown to cause obesity and systemic inflammation in the recipients [11, 12]. In addition, high-fat diet (HFD)-induced symptoms of obesity, insulin resistance, and steatosis were shown to be suppressed in GF mice compared with those in conventional (CONV) mice [13, 14]. It has also been reported that the systemic inflammation associated with aging as observed in CONV mice was attenuated in GF mice [15]. These reports have drawn attention to the role of the gut microbiota in aging, but little is currently known about the mechanisms underlying gut microbiota colonization and aging.

Intestinal bacteria not only provide the host with metabolites but also affect the host's metabolic functions, thereby influencing its lipid profile [16, 17]. The liver is the primary organ where metabolites absorbed from the intestinal tract through the portal vein are processed. Consequently, liver function is largely influenced by the gut ecosystem. It has been demonstrated that, in GF mice, there is a reduction in de novo hepatic lipogenesis and changes in the composition of fatty acids [16, 17]. In GF mice, the lack of gut microbiota results in the disruption of feedback control mechanisms regulating bile acid production [18]. In addition, sexual dimorphism has been observed in the hepatic expression of metabolic enzymes and in the gut microbiota, which may affect not only the lipid profile of the host but also the physiology and pathophysiology of the liver resulting from dysbiosis [4, 19–21]. Nevertheless, the potential link between the colonization of gut microbiota in males and females and the age-related change of the liver remains poorly understood.

Recently, we conducted a comprehensive analysis of the lipidomic profiles associated with aging in SPF and GF mice across a wide range of biological samples including the kidney and liver [22]. Consequently, we identified several aging-associated lipid profiles that exhibited sex- and microbiota-dependent alterations. Here, we aim to elucidate the impact of gut microbiota colonization on gene expression and lipid metabolism during the aging process, with a particular focus on the liver.

Materials and methods

Animal experiment

All animal experiments were performed in accordance with the protocol that was ethically approved by the RIKEN Center for Integrative Medical Sciences [AEY2023-002(9)]. Four-week-old male and female C57BL/6 N mice were purchased from CLEA (Tokyo, Japan). The GF mice were housed in GF isolators at the RIKEN Animal Facility. All mice were fed with an AIN-93 M diet (CLEA Japan, Tokyo, Japan). The mice were the same individuals used for lipidomic analysis as previously reported [22]. Liver tissues were snap-frozen in liquid nitrogen and stored at -80°C until RNA preparation.

RNA sequencing (RNA-seq) analysis

Tissue samples were homogenized in TRIzol reagent (Thermo Fisher Scientific, MA, USA). After centrifugation, the supernatant was collected (500 μL), to which 100 μL of chloroform was added. The mixture was centrifuged, and 150 μL of the obtained supernatant was mixed with 150 μL of 70% ethanol. The total RNA was then extracted using the RNeasy Mini Kit (Qiagen, Hilden, Germany), in accordance with the manufacturer's instructions. A quality check of the RNA was performed using the Agilent RNA 6000 Nano Assay kit (Agilent Technologies, CA, USA) with an Agilent 2100 bioanalyzer to determine the RNA integrity number (RIN) (with an average of 8.8). Subsequently, 100 ng of total RNA was used for library preparation with the NEB Next Ultra RNA Library Prep Kit for Illumina (New England Biolabs, Inc., MA, USA). The pooled libraries were sequenced on an Illumina HiSeq 2500 (Illumina, Inc., CA, USA) at the RIKEN IMS sequence facility, and 50 bp single-end reads were generated. The reads were aligned using STAR onto a mouse reference genome based on UCSC_mm10 [23]. The resulting count matrix was analyzed with edgeR (version 3.42.4) [24]. Genes were filtered out if they did not meet the criterion of >1 count per million in at least three samples prior to differential expression analysis. The false discovery rate (FDR) was corrected by the Benjamini-Hochberg (BH) method. The transcriptomic dataset is presented in Supplementary Table 1.

Gene set enrichment analysis (GSEA)

Normalized expression data were examined by GSEA software (version 4.3.3) (Broad Institute, <http://software.broadinstitute.org/gsea>) using MSigDB (version 2024.1.Mm) [25]. The number of permutations was set to 1000. Gene sets with an FDR < 0.05 were considered to be statistically significant.

Transcription factor analysis

Enrichment of transcription factor binding on the gene promoters was analyzed using ChIP-Atlas (<https://chip-atlas.org>) [26]. In Enrichment Analysis of ChIP-Atlas, we input the 24-month-old female GF differentially expressed genes (DEGs) as dataset A or 24-month-old female SPF DEGs as dataset B and selected “*M. musculus* (mm10),” “ChIP: TFs and others,” “Liver,” and “100” as a threshold. For other settings, we used the default parameters. The fold-enrichment scores of transcription factors with predicted binding to one or more gene sequences with the highest peak count and with a *Q*-value of less than 0.05 are displayed in a heat map.

Reanalysis of lipid profile data

Lipid profile data associated with liver aging were obtained from our previous study and reanalyzed [22]. Briefly, the lipidomic data refer to 771 lipid species belonging to 64 lipid subclasses in 2-, 12-, 19-, and 24-month-old, male/female, SPF/GF mouse samples obtained by the MS-DIAL version 4.20 algorithm. Unpaired *t*-test or one-way analysis of variance followed by Tukey’s test was used to evaluate the significance of differences between two groups or among three or more groups, respectively. The numerical value appended to each lipid molecular species serves to discriminate metabolites sharing the same annotation but exhibiting different retention times.

Statistical analysis and data visualization

Statistical analysis and data visualization were performed using R Studio (version 4.3.0) or Prism (version 9.5.1). The function “prcomp” using the autoscaling method was

employed for principal component analysis (PCA). The function “EnhancedVolcano” was used to create volcano plots of the results of transcriptomic analysis. The normalized values were converted to *z*-scores and heatmaps were drawn using the “heatmap.2” function. Data are presented as mean ± standard error of the mean (SEM) and *P* or FDR < 0.05 is considered to represent statistical significance unless otherwise stated in the figure legends.

Results

The impact of gut microbiota on the liver transcriptome during aging

To investigate the overall effect of gut microbiota on liver aging, we performed RNA-seq analyses using liver samples from young (2 months old: 2 M) and aged (24 months old: 24 M), male and female, SPF and GF mice. PCA using autoscaled values was performed to examine the major variance of the dataset (Fig. 1A). In the young group (2 M), a clear separation between males and females was observed, but obvious differences were not seen between SPF and GF in each sex, and the data mapped with a high degree of clustering within each group (indicated by the same-colored shapes within the circle). These results suggest that the liver transcriptome at a young age is strongly influenced by sex differences rather than gut microbial colonization. Aging resulted in a clear separation between young and aged in each group (male SPF, male GF, female SPF, and female GF), indicating that the transcriptome changes with age. Interestingly, whereas little separation was observed between SPF and GF in the male groups, clear separation was observed in the female groups. We examined the expression of genes reported to increase with age in the mouse liver in each group [27, 28]. The results showed that *Lcn2* and *Clec7a* expression significantly increased with age in male SPF, male GF, and female SPF, but the expression levels in female GF were comparable between young and aged (Fig. 1B). These results suggest that the RNA-seq dataset is reliable and that aging-associated transcriptomic changes are suppressed in female GF mice compared with those in SPF mice.

(See figure on next page.)

Fig. 1 Interpretation of liver transcriptomic data. **A** PCA score plot from liver transcriptomic data based on 13,704 present genes. Data normalization was conducted with the edgeR package, and autoscaling was used for data transformation. Each point in the graph represents a sample ($n = 3$, biologically independent samples). **B** Normalized expression levels of selected hepatic aging-associated genes from the RNA-seq dataset. Data are presented as mean ± SEM ($n = 3$). Significance levels: *FDR < 0.05, **FDR < 0.01. **C** Volcano plots showing young [2-month-old (2 M)] versus aged [24-month-old (24 M)] comparisons in male SPF, male GF, female SPF, and female GF. The *x*- and *y*-axes show the \log_2 [fold change (24 M/2 M)] and $-\log_{10}$ (FDR), respectively. The dashed line indicates 2-fold (*x*-axis) or FDR = 0.05 (*y*-axis). The red circle indicates differentially expressed genes. The numbers of upregulated and downregulated genes are shown in each graph ($n = 3$). **D, E** Venn diagram showing commonly upregulated and downregulated genes during aging in SPF (**D**) and GF (**E**) mice, compared between male and female groups. **F, G** GSEA of liver gene expression during aging in male and female mice under SPF (**F**) or GF (**G**) conditions. The normalized enrichment scores of the top three significantly enriched gene ontology terms are shown (FDR < 0.05)

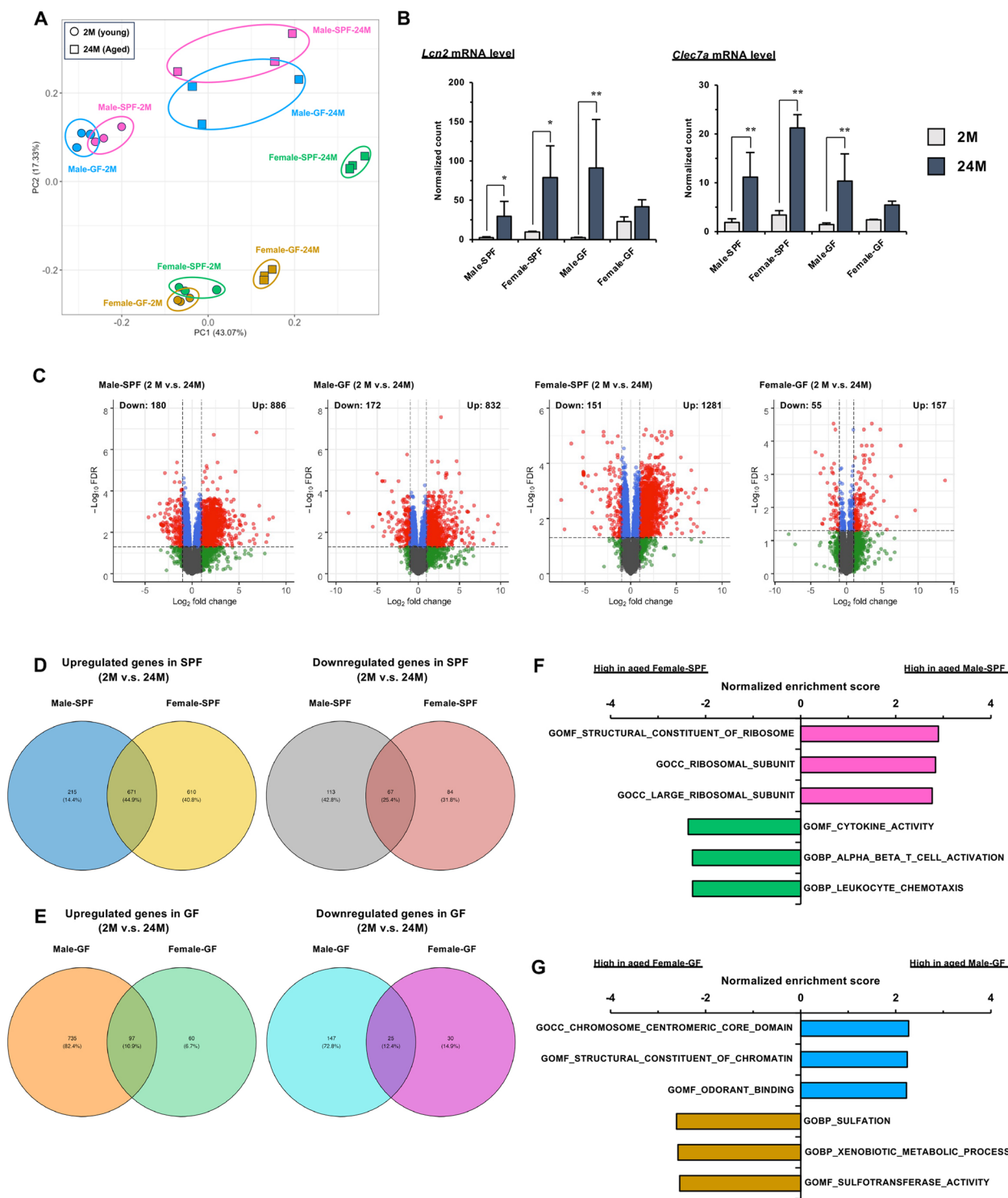


Fig. 1 (See legend on previous page.)

Next, we used a volcano plot to show the changes in gene expression between young and aged mice in the four groups. Using a significance level of 2-fold change (increase or decrease) and $FDR < 0.05$, we found a total

of 1066 DEGs, of which 886 and 180 genes presented increased and decreased expression, respectively, in male SPF mice (Fig. 1C, Supplementary Table 2). Similarly, in male GF mice, the total number of DEGs

was 1004, with 832 genes showing increased expression and 172 genes showing decreased expression. In female SPF, 1432 genes were differentially expressed, with 1281 upregulated and 151 downregulated. In female GF, the number of DEGs was lowest at 212, with 157 upregulated and 55 downregulated. In both male and female SPF mice, 671 DEGs were commonly upregulated and 67 were commonly downregulated with aging (Fig. 1D, Supplementary Table 3). Similarly, in GF mice, 97 DEGs were commonly upregulated and 25 were downregulated (Fig. 1E, Supplementary Table 3). In SPF mice, genes commonly upregulated in both sexes included many inflammation-related genes in SPF mice, such as Toll-like receptors, chemokines, immune cell markers, and immunoglobulins. Although a reduced number of such genes was observed in GF mice, upregulated genes also included immune cell markers and immunoglobulins (Supplementary Table 3). Genes commonly downregulated in both sexes included members of the *Mup*, *Serpina*, and *Ces* gene families under both SPF and GF conditions (Supplementary Table 3). To investigate sex-specific transcriptomic changes associated with aging, GSEA was performed in aged SPF and GF mice. In aged SPF mice, ribosome-related gene sets were significantly enriched in males, whereas inflammatory response-related gene sets were enriched in females, reflecting sex-dependent differences in age-related gene expression at late life stages (Fig. 1F). By contrast, GF mice exhibited a different pattern: chromatin-related gene sets were enriched in males, while xenobiotic metabolism-related gene sets were enriched in females (Fig. 1G). These findings suggest that, although some gene expression changes are shared between sexes, aging-associated transcriptomic alterations differ between males and females, and that the influence of the gut microbiota on these changes is also sex-dependent.

Comparison of hepatic transcriptome between SPF and GF-aged female mice

To characterize the effects of gut microbiota on aging, we compared gene expression between SPF and GF-aged mice. As shown in the volcano plot, there were a total of 742 DEGs in female mice, of which 636 genes were highly expressed in SPF and 106 genes in GF (Fig. 2A, Supplementary Table 4). As shown in Fig. 2B, when the top 25 genes in female mice for both high in SPF and high in GF were depicted in a heatmap, many genes highly expressed in aged SPF were known to be associated with inflammation, especially those related to chemokines (*Ccl3*, *Ccr3*, *Cxcl13*, *Pf4*) and acting as immune cell markers and being related to immune cell functions (*Alox5*, *Batf*, *Cd4*, *Clec10a*, *Eomes*, *H2-M2*, *Ighg1*, *Klra3*, *Mgl2*, *Sh2 d1b1*). *Serpine1*, also known as plasminogen activator inhibitor-1, a marker of cellular senescence, was also upregulated [1, 29]. The expression of these genes was found to increase with age in SPF mice but did not show significant changes in GF mice, indicating that the aging-associated inflammatory signature was ameliorated in these mice. Most of the genes that exhibited high expression in aged GF mice compared to aged SPF mice belonged to the *Mup*, *Sult3a*, and *Fmo* families. The expression of these genes decreased with age in SPF mice, but this trend was less pronounced in GF mice. Conversely, a total of five DEGs were identified in aged male mice. Among these, one gene was highly expressed in aged SPF mice, whereas the remaining four were higher in aged GF mice (Fig. 2C, Supplementary Table 5). These five DEGs were illustrated in a heatmap (Fig. 2D). Notably, *Csad* (a gene involved in metabolism), *Gpx6* (involved in the redox system), and *Neb* (associated with actin filament structure) exhibited similar expression patterns in aged female mice. These findings suggest that the impact of microbiota colonization on gene expression during aging is more pronounced in female mice compared to males.

We further investigated the association between aged SPF and GF female mice by GSEA to identify pathways

(See figure on next page.)

Fig. 2 Comparison of SPF and GF transcriptomes in aged females. **A** Volcano plots showing aged SPF versus aged GF comparisons in female mice. The x- and y-axes show the \log_2 [fold change (GF/SPF)] and $-\log_{10}(\text{FDR})$, respectively. The dashed line indicates 2-fold (x-axis) or $\text{FDR} = 0.05$ (y-axis). The red circle indicates differentially expressed genes. The number of upregulated genes in SPF or GF is shown ($n = 3$). **B** Heatmap of the top 25 genes differentially expressed between SPF and GF in aged female mice (for both high in SPF and high in GF). The expression data for the young age group are also shown. Red, high expression; white, neutral expression; blue, low expression ($n = 3$). **C** Volcano plots showing aged SPF versus aged GF comparisons in male mice. Plot settings are identical to those in panel **A** ($n = 3$). **D** Heatmap of the differentially expressed genes between SPF and GF in aged male mice. The expression data for the young age group are also shown. Color scale and data display are as described in panel **B** ($n = 3$). **E, F** GSEA of liver gene expression in GF compared with SPF in aged female mice. The values of the normalized enrichment score of the significantly enriched gene ontology terms are shown ($\text{FDR} < 0.05$). Upregulated gene sets in SPF and GF are shown in panels **E** and **F**, respectively. **G** Heatmap of the fold enrichment score of transcription factors that regulate the genes differentially expressed between aged female GF and SPF mice, based on the ChIP-Atlas database. The score serves as an indicator of the extent of enrichment of transcription factor binding in the genome of aged female GF mice, in comparison with SPF. The terms that showed a Q-value of less than 0.05 are depicted

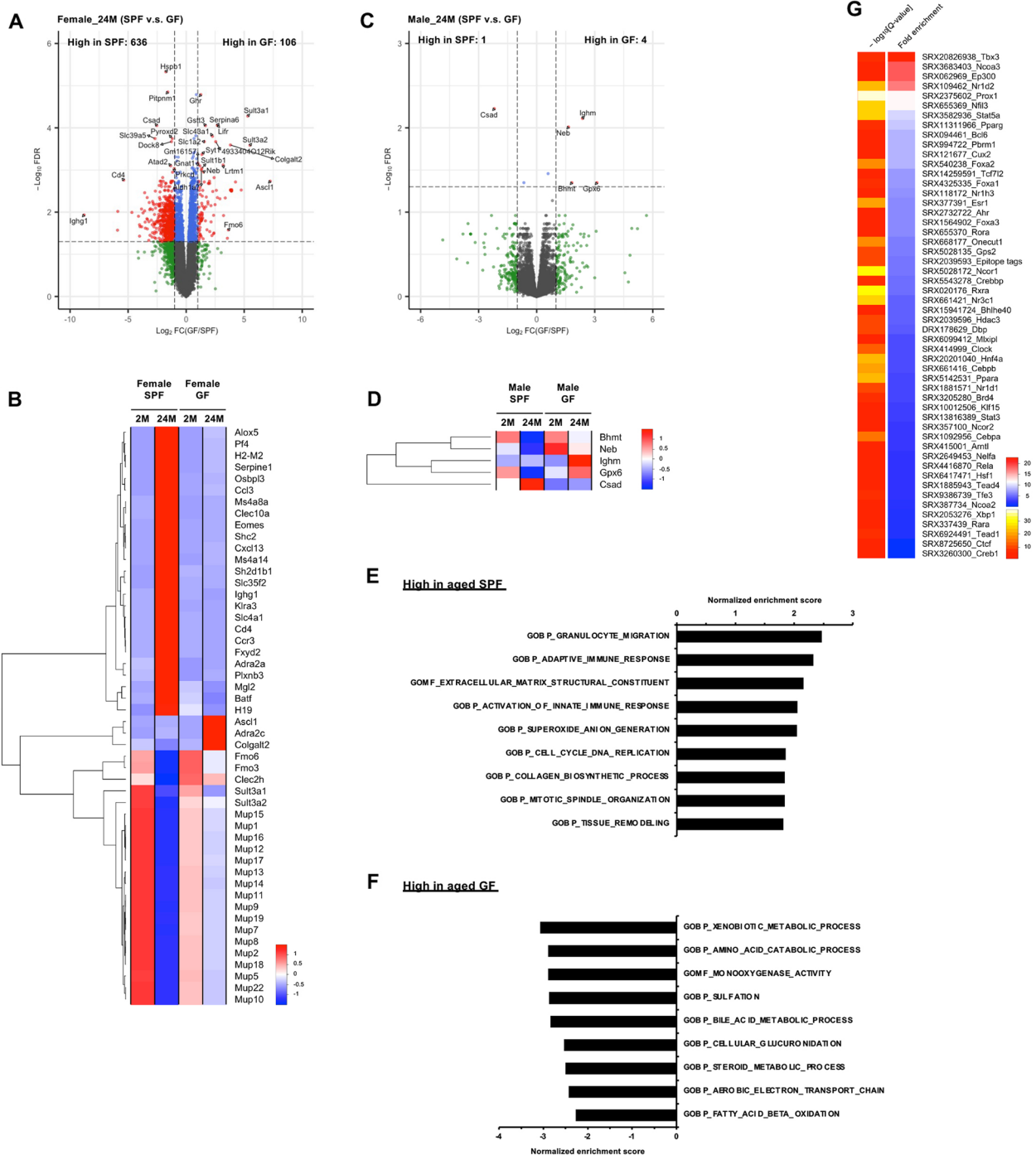


Fig. 2 (See legend on previous page.)

affected by the gut microbiota during the aging process. In SPF mice, in addition to the gene sets related to inflammation (granulocyte migration, adaptive immune response, activation of innate immune response), genes related to tissue remodeling (extracellular matrix structural constituent, collagen biosynthetic process, tissue

remodeling), cell proliferation (cell cycle DNA replication, mitotic spindle organization), and oxidative stress (superoxide anion generation) were enriched in SPF mice compared with the status in GF mice (Fig. 2E). Meanwhile, gene sets involved in xenobiotic metabolism (xenobiotic metabolic process, monooxygenase

activity, sulfation, cellular glucuronidation), amino acid metabolism (amino acid catabolic process), cholesterol metabolism (steroid metabolic process), and bile acid metabolism (bile acid metabolic process) were enriched in GF mice compared with the status in SPF mice (Fig. 2F). Moreover, gene sets involved in mitochondrial energy production (aerobic electron transport chain, fatty acid β -oxidation) were also enriched in GF compared with those in SPF mice, reflecting the suppression of the decline in mitochondrial energy production with age [1, 28].

We analyzed upstream transcription factors corresponding to the differential gene expression signature between SPF and GF in the livers of aged female mice, based on the previously reported ChIP-Seq (chromatin immunoprecipitation sequencing) datasets using ChIP-Atlas [26]. This *in silico* analysis predicted the transcription factors Stat5a, Bcl6, Cux2, HNF4a, Esr1, Foxa1, and Foxa2, which have been implicated in sex differences, as key transcription factors in the livers of aged female GF mice (Fig. 2G, Supplementary Table 6) [30–33]. In addition, Ppara and Pparg, which are associated with lipid metabolism and mitochondrial function, emerged as key factors in aged GF mice [34]. In contrast, the involvement of Rela, a component of nuclear factor- κ B (NF- κ B) and Tfe3, both of which are important in regulating inflammatory cytokine expression, was predicted in the livers of aged female SPF mice [35, 36]. Unlike in females, transcription factor prediction using ChIP-Atlas was not feasible in aged male mice due to the limited number of DEGs between SPF and GF conditions. The results indicate that various aging-associated functional abnormalities, including those related to metabolism and energy production, as well as inflammatory signatures, are suppressed in female GF compared with the levels in SPF mice. The results also suggest that both sex-associated transcription factors and those not previously linked to sex differences may be involved in the regulation of these pathways observed in females.

The impact of colonization of gut microbiota on hepatic lipid metabolism in aged female mice

The discrepancies in the aging process between female SPF and GF mice are assumed to involve functions that regulate aging-related phenotypes, such as inflammatory response. To clarify the potential link between the regulation of aging by gut microbiota and host lipid metabolism, we reanalyzed our previously reported aging lipidome atlas datasets and compared the hepatic lipid profiles between SPF and GF in aged female mice (Fig. 3A, Supplementary Table 7) [22]. A volcano plot with a threshold of $P < 0.05$ revealed that 10 species in 7 subclasses were more abundant in SPF and 54 species in 18 subclasses were more abundant in GF. The molecular species that met the criteria are displayed in a heatmap (Fig. 3B). Of these, bile acid BA 24:1;O3;T (taurodeoxycholic acid: TDCA) (ID 1690), BA 24:1;O4;T (ID 1776), BA 24:1;O2;T (ID 1594), and BA 24:1;O3;T (ID 1697) increased with age in SPF mice, while remaining at low levels in GF mice. In contrast, BA 24:1;O4;T (ID 1780) remained at a low level in SPF mice and at a high level in GF mice. Primary bile acids produced by the host from cholesterol are metabolized by gut microbiota to secondary bile acids. The level of TDCA, a secondary bile acid, remained low in GF mice, a finding that appears to support the reliability of these lipid profiles. Sterol sulfate (SSulfate) is a lipid subclass in which the sterol structure is sulfated by sulfotransferases (Sults) [37, 38]. Within this lipid subclass, the levels of ST 27:1;O;S (ID 1528) and ST 27:0;O;S (ID 1539) were consistently higher in GF than in SPF from young to old age. The species classified as lysophosphatidylcholine (LPC), lysophosphatidylethanolamine (LPE), vitamin D, and phytoceramide (Cer_{NP}) increased with age in GF mice, and the levels were significantly higher than those in SPF mice at old age [LPC 16:1/0/0 (ID: 1926), LPE 16:0 (ID: 1749), LPE 17:0 (ID: 1831), 25-hydroxycholecalciferol (ID: 1428), and Cer 18:0;3O/24:1 (ID: 3068)], whereas no age-dependent changes were observed in SPF. Similarly, a total of 26 lipid molecular species of oxidized

(See figure on next page.)

Fig. 3 Comparison of SPF and GF lipidomes in aged female mice. **A** Volcano plots showing aged SPF versus aged GF comparisons in female mice. The x- and y-axes show the \log_2 [fold change (GF/SPF)] and $-\log_{10}(P\text{-value})$, respectively. The dashed line indicates $P\text{-value} = 0.05$ (y-axis). The circle indicates lipid species. The number of lipid species with significant change between aged SPF and aged GF mice is shown for each lipid subclass ($n = 3$). **B** Heatmap of the lipid species showing significant change between SPF and GF in aged female mice. Data for the young age group are also shown. Red, high levels; white, neutral levels; blue, low levels. The lipid species with a statistically significant difference between the levels in SPF and GF mice are marked with an asterisk in 2-month-old (2 M) and 24-month-old (24 M) groups. The significance of differences between 2 M and 24 M is also shown in the heatmap boxes for SPF and GF ($n = 3$). Significance levels: * $P < 0.05$, ** $P < 0.01$, *** $P < 0.001$. **C** Volcano plots showing aged SPF versus aged GF comparisons in male mice. Plot settings are identical to those in panel **A** ($n = 3$). **D** Heatmap of the lipid species showing significant change between SPF and GF in aged male mice. Data for the young age group are also shown. Color scale and data display are as described in panel **B** ($n = 3$). Significance levels: * $P < 0.05$, ** $P < 0.01$, and *** $P < 0.001$

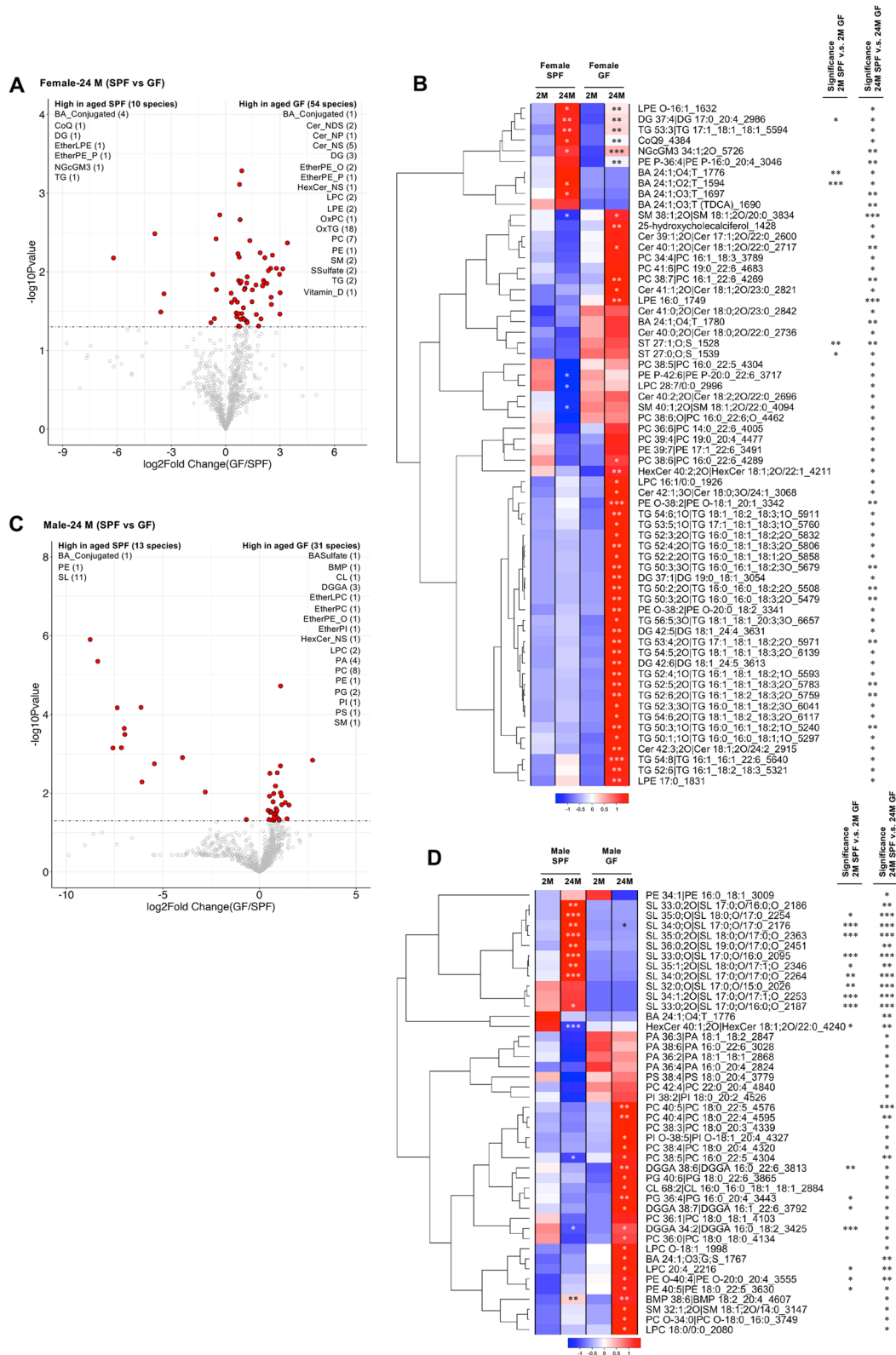


Fig. 3 (See legend on previous page.)

triacylglycerol (oxTG) were detected, and 18 of them, such as TG 18:1_18:2_18:3;1O (ID 5911), increased with age in GF and showed higher levels in GF than in SPF in the aged mice. Moreover, unique changes in acyl groups were observed in phosphatidylcholine (PC), ceramide (Cer_NS), dihydroceramide (Cer_NDS), hexosylceramide (HexCer_NS), and sphingomyelin (SM). The level of PC with polyunsaturated fatty acid (PUFA) 22:6 was significantly higher in aged GF than in SPF, and PC 16:0_22:6 (ID 4289) and PC 16:1_22:6 (ID 4269) significantly increased with age in GF mice. In addition, the levels of sphingolipid molecular species with fatty acids with 22 to 23 carbons as the *N*-acyl group were significantly higher in aged GF than in SPF, and among them, Cer 18:1;2O/22:0 (ID 2717), Cer 18:1;2O/23:0 (ID 2821), and HexCer 18:1;2O/22:1 (ID 4221) increased with age in GF. These changes are the hepatic lipidomic signature differentiating SPF and GF in aged female mice, and the colonization of gut microbiota may be the driving factor behind these differences. Conversely, although two molecular species, BA 24:1;O4;T (ID: 1776) and PC 16:0_22:5 (ID: 4304), were identified as common lipidomic alterations between aged SPF and GF mice of both sexes, most lipidomic differences between aged SPF and GF mice were sex-specific (Fig. 3C, Supplementary Table 8). In aged males, characteristic differences between SPF and GF mice included phosphatidic acid (PA), PC species containing 18:0 and PUFA, and diacylglycerol glucuronide (DGGA), as well as sulfonolipid (SL), a gut microbiota-dependent lipid species we previously reported [22] (Fig. 3D). Although a similar trend in SL levels was observed in aged females, greater inter-individual variability compared to males prevented the detection of statistically significant differences. The significances observed in this analysis may partially reflect differences in abundance variations in aged mice. These lipidomic differences between aged SPF and GF mice may underlie the observed sex differences in transcriptomic changes associated with aging.

Integration of the hepatic transcriptome and lipidome in female mice

Next, we integrated the transcriptomic and lipidomic datasets and mapped the possible lipid metabolic pathways involved in the lipidomic changes between SPF and GF-aged female mice according to the public KEGG pathway map database (<https://www.kegg.jp>) and previous reports. The *Sult2* family is a group of hydroxysteroid sulfotransferases that are involved in the production of sterol sulfate (Fig. 4A) [37]. As shown in Fig. 2E, the gene set related to sulfation was enriched in GF mice compared to SPF mice. The expression levels of about half of the *Sults* increased with aging in GF mice and were higher than in aged SPF mice, suggesting that these *Sults* are involved in the accumulation of sterol sulfate in the liver of GF mice (Fig. 4B). Cer_NDS undergoes C4 hydroxylation to yield Cer_NP, which in turn undergoes degradation to phytosphingosine (Fig. 4C). It has been proposed that *Degs1*, *Degs2*, and *9130409I23Rik* are involved in the abovementioned production pathway, while *Asah1*, *Asah2*, and *Acer3* are associated with the degradation [39]. The expression of enzymes involved in Cer_NP production was comparable between aged SPF and GF (Fig. 4D). However, the level of *Acer3*, involved in degradation, increased with aging in SPF, with higher levels in the aged SPF mice than in the aged GF ones. This may have contributed to the difference in Cer_NP between SPF and GF. The lysophospholipids LPC and LPE are generated by the hydrolysis of PC and phosphatidylethanolamine (PE) by phospholipase A_{1/2} (PLA_{1/2}) and are then remodeled to corresponding phospholipids by lysophospholipid acyltransferase (LPLAT) (Fig. 4E) [40]. In female GF mice, the majority of LPC and LPE species were increased with age (Supplementary Table 9). Although the levels of *Pla2g15* and *Pla2g4f* were elevated during the aging process in GF mice, no significant differences were observed between SPF and GF mice at an old age (Fig. 4F). In contrast, the expression of LPLAT genes, including *Lpcat1* and *Lpcat2*, increased with age in SPF mice, resulting in elevated levels in aged mice relative to those in GF mice, suggesting that these remodeling

(See figure on next page.)

Fig. 4 Aging-associated change in lipid metabolic pathways in female SPF and GF mice. **A** Metabolic pathway of sterol sulfate. **B** Heatmap of the expression levels of the genes encoding sulfotransferase in female 2- and 24-month-old SPF/GF mice. **C** Metabolic pathway of phytoceramide. **D** Heatmap of the expression levels of the genes encoding phytoceramide metabolic enzymes in female 2- and 24-month-old SPF/GF mice. **E** Metabolic pathway of lysophospholipid and phospholipid metabolism. **F** Heatmap of the expression levels of the genes encoding phospholipid metabolism in female 2- and 24-month-old SPF/GF mice. **G** Metabolic pathway of 22:6-containing phospholipid metabolism. Quantification of each lipid subclass was performed by summing the values of each lipid molecule classified in the lipid subclasses (A, C, E, G, and Supplementary Table 7). *P* values were calculated using Tukey's test for lipid analysis or *t*-test for gene expression analysis. Genes with a statistically significant difference between the levels in SPF and GF are marked with an asterisk in female 24 M mice. The significance of differences between 2 M and 24 M is also shown in the heatmap boxes for SPF and GF. Significance levels: **P* < 0.05, ***P* < 0.01, and ****P* < 0.001 (*n*=3)

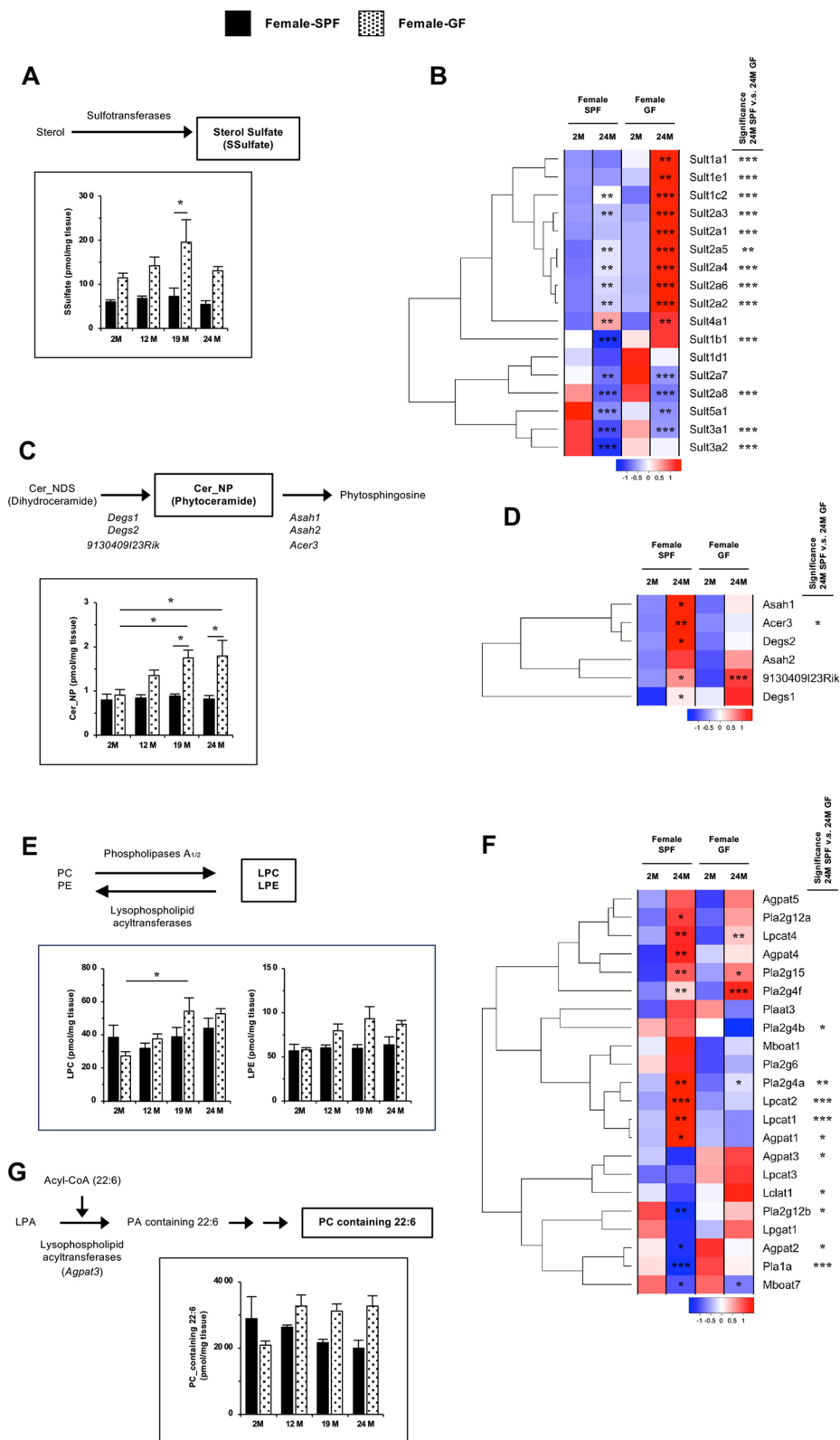


Fig. 4 (See legend on previous page.)

enzymes are responsible for the accumulation of LPC and LPE in GF mice. The quality of phospholipids is regulated by the acyl chain preferentiality of LPLAT [40]. *Agpat3*, which is known to preferentially introduce 22:6 into lysophosphatidic acid (a common precursor of phospholipids) in mouse liver, tends to maintain a higher expression level in GF than in SPF and was markedly more highly expressed in aged GF than in SPF (Fig. 4F and G) [41]. The expression of this enzyme may explain the profile of 22:6-containing PCs.

Discussion

In this study, we found that the gut microbiota affected the changes in the liver transcriptome associated with aging in mice. Female GF mice exhibited attenuated changes in the aging-associated transcriptome, such as inflammatory signatures, compared with those in SPF mice. As an explanation for this, it was predicted that female GF mice may exhibit enhanced regulation of gene expression via sex-related transcription factors. Furthermore, the integrated transcriptomic and lipidomic analysis in female mice suggested that lipid metabolism in the liver was altered in a manner dependent on the gut bacteria, which may be involved in controlling aging-associated phenotypes, including inflammation. These results offer new insights into the molecular mechanisms through which the gut microbiota regulates liver aging. In particular, sex differences and lipid metabolism may be involved in this process.

Transcriptomic analysis revealed differences in the aging-associated inflammatory signatures in the liver between female SPF and GF mice. Upregulation of gene sets related to the extracellular matrix and tissue remodeling in female SPF indicates abnormal tissue repair, suggesting that chronic inflammation leads to liver fibrosis, cirrhosis, and liver failure [42]. The infiltration of immune cells and the increase in myofibroblasts, which are extracellular matrix-producing cells, play an important role in the progression of these diseases [43, 44]. Since these cells are highly proliferative, the fact that the gene set related to cell proliferation was upregulated in aged SPF mice may be attributed to the proliferation of these cells [43, 44]. Based on these results, it is suggested that the colonization of gut microbiota leads to various age-dependent pathological conditions associated with liver inflammation in female mice.

A variety of immune cells reside in the liver and contribute to the maintenance of hepatic homeostasis [45]. Previous studies have reported no significant differences in the number of leukocytes or the proportions of natural killer T (NKT) cells and dendritic cells in the livers of female SPF and GF mice under steady-state conditions [46]. Consistently, our transcriptomic analysis

revealed no differences in the expression of immunity-related genes between SPF and GF mice in young females (Supplementary Table 3). In mouse models of steatosis, immune cells such as T cells, B cells, macrophages, Kupffer cells, and NKT cells are known to be involved in disease pathogenesis [47–51]. In the Concanavalin A-induced hepatitis model, more severe acute liver inflammation has been observed in SPF female mice compared to GF mice, which has been attributed to the activation of hepatic NKT cells by gut microbiota-derived glycolipid antigens, such as α -galactosylceramide and subsequent decline in the frequency of hepatic NKT cells [46]. In contrast, in the context of HFD-induced obesity and hepatic metabolic dysfunction, NKT cells appear to play a protective role, as female mice lacking NKT cells exhibit increased susceptibility to these metabolic disturbances [52]. In both humans and mice, aging has been reported to be associated with a decline in hepatic NKT cell number and functions [53]. Unlike GF mice, NKT cells in SPF mice are continuously activated in a gut microbiota-dependent manner, which may be associated with their age-related decline. In contrast, in the absence of gut microbiota, NKT cell function may be preserved even in old age, potentially leading to the suppression of aging-associated liver inflammation. Our current lipidomic analysis did not identify specific lipid species that regulate NKT cells, highlighting the need for more detailed lipidomic profiling to address this possibility. Collectively, these findings suggest a potential role for gut microbiota-mediated regulation of NKT cells and other immune cells in the development of age-associated liver disorders, highlighting the need for further studies.

In female mice, the aging-associated inflammatory signature in the liver was reduced in GF compared to SPF mice, suggesting that gut microbiota progress to aging-related inflammation. Consistently, fecal transplantation from aged female SPF mice into young female GF mice has been shown to induce systemic inflammation, whereas transplantation from young SPF mice did not, indicating that aged microbiota may harbor pro-inflammatory factors [11]. Aging-associated dysbiosis has been proposed to increase intestinal permeability, allowing microbial products to enter circulation and trigger inflammation [11, 15]. The absence of such gut-derived factors may underlie the suppressed inflammation observed in female-aged GF mice. Notably, in aged male mice, liver transcriptomic differences between SPF and GF were less pronounced, suggesting that age-related inflammation in males may occur independently of the gut microbiota. Alternatively, certain yet unidentified microbiota-derived lipids may possess anti-inflammatory properties, which could confer protection in male mice. These findings underscore the importance of considering

sex differences in understanding the relationship between gut microbiota and age-related inflammation. The observed sex-specific differences in transcriptomic and lipidomic profiles offer new insights into the regulation of aging-related inflammation.

Our ChIP-Atlas-based analysis of transcription factors suggests that a group of transcription factors related to sex differences may be involved in the aging-associated gene expression in female GF mice [26]. The liver exhibits sexual dimorphism that is achieved by certain sex-related transcription factors, such as Stat5a, Bcl6, Cux2, and HNF4 α , which are regulated by growth hormone (GH) secreted from the pituitary gland [54–58]. These transcription factors regulate the expression of various metabolic enzymes and affect the metabolism of lipids, steroids, and xenobiotics [30, 31, 59]. For example, it was shown that mice with Bcl6 deficiency specifically in hepatocytes exhibit resistance to HFD-induced steatosis, observed in both male and female mice, although the tendency is more pronounced in male mice [60]. Bcl6 plays a pivotal role in the repression of female-biased genes in males [57]. Hepatocyte-specific deletion of Bcl6 results in the feminization of the male liver and the elimination of its male-biased gene signature [60]. Meanwhile, the expression of *Cyp3a41*, *Cyp3a44*, and *Mup* genes, which are known to be regulated by GH through sex-related transcription factors, was higher in GF than in SPF in aged female mice [61, 62]. This indicates that the age-related decline in the GH-dependent transcriptional axis is suppressed in female GF mice, thereby preventing age-related abnormalities in the liver. The secretion of GH is influenced by a variety of hormones [63]. However, it has been reported that changes in GH secretion in GF mice compared with that in CONV mice resulted in the attenuation of sex-specific diurnal rhythms of gene expression and metabolism [64]. Furthermore, it has been postulated that microbiota-derived short-chain fatty acids, such as butyrate, are involved in the regulation of GH secretion, suggesting the existence of gut microbiota-dependent regulatory mechanisms [65]. Clarifying the role of the gut microbiota in GH-dependent function in aged mice may help to elucidate how the gut microbiota is involved in the differences in liver aging between the sexes.

There are also differences in liver physiology and pathology between the sexes, such as in the induction of MAFLD by HFD feeding. It has been reported that symptoms are more pronounced in males than in females [21, 30]. In female mice, sex hormones can suppress inflammation and alter various metabolic processes. It has been reported that estrogen administration reduces inflammation and HFD-induced steatosis in mice [31, 66, 67]. In addition, estrogen is known to protect the liver from xenobiotic stimuli by increasing the expression of

enzymes such as cytochrome P450, and sulfotransferase in the liver, as observed in aged female GF mice [21, 31, 68]. Furthermore, our analysis of transcription factors suggests that in addition to *Esr1*, *Foxa1*, and *Foxa2* were also functional in aged female GF mice. *Foxa1/2* has been implicated in the sexual dimorphism of hepatocarcinogenesis. It has been reported that liver cancer could be prevented by the estrogen-dependent expression of genes involved in xenobiotic metabolism and proliferation in female mice, which was dependent on *Foxa1/2* [33]. It is thus proposed that estrogen-dependent protective mechanisms are involved in the process by which the livers of female GF mice are protected from the aging-associated inflammatory response.

It is also possible that xenobiotic enzymes are induced to produce metabolites with endogenous anti-inflammatory properties. The predominant molecular species of SSulfate annotated in this study, ST 27:1;O;S (ID: 1528), is predicted to be a cholesterol sulfate (CS). CS has been reported to have anti-inflammatory effects in vitro and in vivo [38, 69, 70]. Therefore, the increase in CS is thought to be involved in the suppression of age-related inflammation observed in GF mice. CS is known to be produced by *Sult2b1b*, expressed in the intestinal epithelium [69, 71]. In addition to *Sult2b1b*, it has been suggested that *Sult2a1*, albeit with less specificity, is also involved in the production of CS [37, 71]. It has been observed that the *Sult2a* gene exhibits higher levels of expression in female mice than in male ones. This sexual dimorphism in *Sult2a1* expression in mouse livers is regulated by sex hormones, estrogen in females, and GH [68]. According to the ChIP-Atlas database, there are potential binding sites of the sex-related transcription factors *Esr1*, *Foxa1*, *Foxa2*, *Stat5a*, and *HNF4 α* within a region spanning ± 1 kb from the transcription start site of the *Sult2a1* gene. This suggests that the production of CS via the upregulation of *Sult2a1* improves the liver pathology associated with aging in a sex-dependent manner. However, further analysis is needed to elucidate the potential mechanism by which SSulfate increases in female GF mice and to clarify its role in liver inflammation.

The results of the integrated transcriptomic and lipidomic analysis revealed unique differences in lipid metabolism between SPF and GF, which may regulate inflammation in the liver during aging. Phytoceramide is produced by the C4-hydroxylation of dihydroceramide. Previous reports suggested *DeGs2* as the enzyme responsible for this reaction, but the fact that phytoceramide was not completely abolished by *DeGs2* deficiency suggests that other enzymes produce it [72, 73]. The KEGG pathway map suggests the possible involvement of the enzyme encoded by *9130409I23Rik*, also called *DeGs1 l*,

in this reaction. Our findings indicate that the elevation of phytoceramides in GFs is attributable to discrepancies in the degradation system rather than the production system between SPF and GF. Although it is not known whether there are sex differences or gut microbiota-dependent differences in the expression of *Acer3*, it has been reported that such expression is increased in non-alcoholic steatohepatitis patients and disease model mice and that inflammation, fibrosis, and oxidative stress in such mice are reduced by *Acer3* deletion [39, 74]. It has also been reported that phytoceramide activates peroxisome proliferator-activated receptors, suggesting their possible role in regulating aging-related phenotypes in the liver [34, 75].

Phospholipids are converted to lysophospholipids by PLA_{1/2} and recycled to the corresponding phospholipids by LPLATs. Based on gene expression analysis, the accumulation of LPC and LPE in aged GF may be due to differences in the expression of the LPLAT genes, *Lpcat1* and *Lpcat2*, which are known to be involved in the acylation of LPC and LPE [40]. LPC and LPE have been reported to act as signaling molecules that control inflammation. LPC is known to have an inhibitory effect on sepsis and Con-A-induced acute hepatitis, while LPE has an inhibitory effect on animal models of inflammation such as peritonitis and edema [76–79]. It has been suggested that these effects differ depending on the position (*sn-1* or *sn-2*) and the type (number of carbons, degree of saturation) of the acyl chain [80, 81]. Using the measurement system employed in our previous study, it is not possible to distinguish the sites where acyl groups are attached [22]. Against this background, there is a need for further analysis to elucidate the molecular mechanisms by which these lipids suppress inflammation associated with liver aging, as well as the potential role of sex differences and gut microbiota in the metabolism of LPC and LPE.

Differences in acyl chain quality have a significant impact on the properties of lipids. In female GF mice, the amount of PC containing 22:6 increased with age and was higher than in aged SPF mice. PUFAs such as 22:6 have a significant impact on the properties of phospholipids, for example, by increasing the fluidity of biological membranes and acting as precursors of lipid mediators that promote the resolution of inflammation [82]. As membrane fluidity declines with age, it is possible that 22:6-containing PC contributes to inhibit this decline [83]. LPLAT plays an important role in the diversity of phospholipid quality. In particular, *Agpat3* incorporates 22:6 into lysophosphatidic acid to produce PA. PA is further metabolized to produce 22:6-containing PC. It has been reported that PC containing 22:6 is significantly reduced in *Agpat3*-deficient mice [40, 41]. To ascertain

whether *Agpat3* expression is modulated by sex-related transcription factors, *in silico* screening of the *Agpat3* promoter was conducted using the JASPAR program (<https://jaspar.elixir.no>) [84]. The consensus sequences in the promoter region of *Agpat3* were screened using the JASPAR program, which resulted in the prediction of high-scoring binding for Bcl6 (ID: MA0463.1, predicted sequence: CTTCTTAGAGAAGA) and Stat5a (ID: MA0519.2, predicted sequence: TTCTTAGAG). These results suggest that the observed increase in *Agpat3* may have contributed to alterations in the PC profile in a sex-dependent manner. Overall, the impact of sex differences and gut microbiota on the expression of metabolic enzymes that contribute to the observed differences in lipid profile remains to be further analyzed to determine the effects of these changes in lipid metabolism on aging-associated phenotypes, including inflammation.

A comprehensive analysis of age-related lipid changes in the liver is limited in humans due to the invasive nature of liver sampling, with most studies focusing on lipids in the blood samples [85, 86]. In contrast, lipidomic analyses using liver biopsies from patients with hepatic diseases such as steatosis and cirrhosis have identified lipid species associated with disease pathology [87]. In this study, we observed age-dependent increases in cholesterol esters, triacylglycerols, and diacylglycerols, as well as decreases in certain sphingolipids in the livers of SPF mice. These changes have also been reported in human liver diseases. These findings suggest that age-related lipid alterations in the mouse liver may reflect features of human age-associated liver disorders. Our results offer insights into age-related lipid metabolic changes in the human liver and may contribute to the future development of biomarkers and therapeutic strategies, including microbiota-targeted interventions such as probiotics, and postbiotics for aging-related liver diseases.

Conclusions

In summary, this study provides substantial insights into the potential link between aging-associated transcriptome and lipidome changes and gut microbiota especially in female mice liver. It is important to elucidate the fundamental mechanisms by which the colonization of gut microbiota affects the process of aging of the host tissue in a sex-dependent manner. Our findings indicate that changes in sex-related hormonal regulation and lipidome changes are a potential mechanism underlying this relationship. Further research is needed to determine the causal relationship between specific gut microbiota and aging-related phenotypes in a sex-dependent manner. This study provides a basis for future work to develop new therapeutic strategies for aging-associated liver diseases.

Abbreviations

BH	Benjamini-Hochberg
Cer_NS	Ceramide
CS	Cholesterol sulfate
ChIP-Seq	Chromatin immunoprecipitation sequencing
CONV	Conventional
DGGA	Diacylglycerol glucuronide
DEGs	Differentially expressed genes
Cer_NDS	Dihydroceramide
FDR	False discovery rate
GSEA	Gene set enrichment analysis
GF	Germ-free
GH	Growth hormone
HexCer_NS	Hexosylceramide
HFD	High-fat diet
LPC	Lysophosphatidylcholine
LPE	Lysophosphatidylethanolamine
LPLAT	Lysophospholipid acyltransferase
MAFLD	Metabolic dysfunction-associated fatty liver disease
NKT	Natural killer T
NF- κ B	Nuclear factor- κ B
oxTG	Oxidized triacylglycerol
PA	Phosphatidic acid
PC	Phosphatidylcholine
PE	Phosphatidylethanolamine
PLA _{1/2}	Phospholipase A _{1/2}
PUFA	Polyunsaturated fatty acid
Cer_NP	Phytoceramide
PCA	Principal component analysis
RIN	RNA integrity number
RNA-seq	RNA sequencing
SL	Sulfonolipid
SPF	Specific pathogen-free
SM	Sphingomyelin
SEM	Standard error of the mean
SSulfate	Sterol sulfate
Sults	Sulfotransferases
TDCA	Taurodeoxycholic acid

Supplementary Information

The online version contains supplementary material available at <https://doi.org/10.1186/s41232-025-00377-2>.

Supplementary Material 1: Supplementary Table 1. Normalized count data of RNA-seq analysis.

Supplementary Material 2: Supplementary Table 2. Gene expression analysis in male/female SPF/GF mice during the aging process (2-month-old vs. 24-month-old) in the liver.

Supplementary Material 3: Supplementary Table 3. List of DEGs commonly upregulated or downregulated with aging in both male and female mice under SPF and GF conditions.

Supplementary Material 4: Supplementary Table 4. Gene expression analysis between SPF and GF in the liver of aged (24M) or young (2M) female mice (SPF vs. GF).

Supplementary Material 5: Supplementary Table 5. Gene expression analysis between SPF and GF in the liver of aged (24M) or young (2M) male mice (SPF vs. GF).

Supplementary Material 6: Supplementary Table 6. Results of the fold enrichment score of transcription factors that regulate the genes differentially expressed between aged female GF and SPF mice, based on the ChIP-Atlas.

Supplementary Material 7: Supplementary Table 7. Results of reanalysis of the changes in liver lipidome (species-level) between SPF and GF in female aged (24M) or young (2M) mice. Values of each molecular species are shown in pmol/mg tissue.

Supplementary Material 8: Supplementary Table 8. Results of reanalysis of the changes in liver lipidome (species-level) between SPF and GF in male aged (24M) or young (2M) mice. Values of each molecular species are shown in pmol/mg tissue.

Supplementary Material 9: Supplementary Table 9. Results of reanalysis of the changes in liver lipidome (species-level) between young (2M) and aged (24M) SPF or GF female mice. Values of each molecular species are shown in pmol/mg tissue.

Supplementary Material 10: Supplementary Table 10. Results of reanalysis of the changes in liver lipidome (subclass-level) during the aging process in SPF or GF female mice (2-month-old, 2M; 12-month-old, 12M; 19-month-old, 19M; 24-month-old, 24M). Values of each lipid subclass are shown in pmol/mg tissue.

Authors' contributions

T.I., H.T., A.M., and M.A. designed the study. T.I. performed experiments. T.I. and J.C. conducted the transcriptomic analysis of the liver. T.I., H.T., and S.I. performed the lipidomic reanalysis of the liver. T.I. and M.A. wrote the manuscript. All authors have thoroughly discussed this project and helped improve the manuscript.

Funding

This work was supported by JSPS Grants-in-Aid for Scientific Research on Innovative Areas "Biology of LipoQuality" (15H05897 and 15H05898 to M.A.), JSPS KAKENHI (22 K11718 to T.I., 24 K02011, 24H00043, 24H00392, and 24 K21269 to H.T., 20H00495 to M.A.), the National Cancer Center Research and Development Fund (2023-A-08, H.T.), AMED Japan Program for Infectious Diseases Research and Infrastructure (21wm0325036 h0001, H.T. and M.A.), AMED Moonshot Research and Development Program (22zf0127007 to M.A.), AMED NeDDTrim (21ae0121036 to M.A.), Suzuken Memorial Foundation (21-070, T.I.), JST National Bioscience Data-base Center (JPMJND2305, H.T.), JST FOREST Program (JPMJFR230H) to H.T., JST ERATO "Arita Lipidome Atlas Project" (JPMJ-JER2101 to H.T. and M.A.), and RIKEN Aging Project Program (M.A. and A.M.).

Data availability

The RNA-seq raw data are available on the DDBJ webpage, under identifier PRJDB 19844. Lipidomic data are available on the RIKEN DROP Met website (http://prime.psc.riken.jp/menta.cgi/prime/drop_index), index number DM0044, or in our published manuscript [22].

Declarations**Ethics approval and consent to participate**

This study was approved by the Animal Committee of the RIKEN Center for Integrative Medical Sciences (permission number: AEY2023-002(9)).

Consent for publication

Not applicable.

Competing interests

The authors declare that they have no competing interests.

Author details

¹Laboratory for Metabolomics, RIKEN Center for Integrative Medical Sciences, 1-7-22, Suehiro-cho, Tsurumi-ku, Yokohama, Kanagawa 230-0045, Japan. ²Faculty of Pharmaceutical Sciences, Nagasaki International University, 2825-7, Huis Ten Bosch, Sasebo, Nagasaki 859-3298, Japan. ³Department of Biotechnology and Life Science, Tokyo University of Agriculture and Technology, 2-24-16 Nakamachi, Koganei-shi, Tokyo 184-8588, Japan. ⁴Metabolome Informatics Research Team, RIKEN Center for Sustainable Resource Science, 1-7-22 Suehiro-cho, Tsurumi-ku, Yokohama, Kanagawa 230-0045, Japan. ⁵Molecular and Cellular Epigenetics Laboratory, Graduate School of Medical Life Science, Yokohama City University, Tsurumi-ku, Yokohama, Kanagawa 230-0045, Japan. ⁶Division of Physiological Chemistry and Metabolism, Graduate School of Pharmaceutical Sciences, Keio University, 1-5-30 Shibakoen, Minato-ku, Tokyo 105-8512, Japan. ⁷Laboratory for Cellular Epigenomics, RIKEN Center for Integrative Medical Sciences, 1-7-22, Suehiro-cho, Tsurumi-ku, Yokohama, Kanagawa 230-0045, Japan. ⁸Department of Human Biology, Radboud

Institute for Molecular Life Sciences, Faculty of Science, Radboud University Nijmegen, Nijmegen, The Netherlands.

Received: 10 January 2025 Accepted: 20 April 2025

Published online: 03 May 2025

References

- Lopez-Otin C, Blasco MA, Partridge L, Serrano M, Kroemer G. Hallmarks of aging: an expanding universe. *Cell*. 2023;186(2):243–78. <https://doi.org/10.1016/j.cell.2022.11.001>.
- Hunt NJ, Kang SWS, Lockwood GP, Le Couteur DG, Cogger VC. Hallmarks of aging in the liver. *Comput Struct Biotechnol J*. 2019;17:1151–61. <https://doi.org/10.1016/j.csbj.2019.07.021>.
- Ghosh TS, Shanahan F, O'Toole PW. The gut microbiome as a modulator of healthy ageing. *Nat Rev Gastroenterol Hepatol*. 2022;19(9):565–84. <https://doi.org/10.1038/s41575-022-00605-x>.
- DeJong EN, Surette MG, Bowdish DME. The gut microbiota and unhealthy aging: disentangling cause from consequence. *Cell Host Microbe*. 2020;28(2):180–9. <https://doi.org/10.1016/j.chom.2020.07.013>.
- Franceschi C, Garagnani P, Parini P, Giuliani C, Santoro A. Inflammaging: a new immune-metabolic viewpoint for age-related diseases. *Nat Rev Endocrinol*. 2018;14(10):576–90. <https://doi.org/10.1038/s41574-018-0059-4>.
- Johnson AA, Stolzing A. The role of lipid metabolism in aging, lifespan regulation, and age-related disease. *Aging Cell*. 2019;18(6):e13048. <https://doi.org/10.1111/acer.13048>.
- Ando A, Oka M, Satomi Y. Deoxysphingolipids and ether-linked diacylglycerols accumulate in the tissues of aged mice. *Cell Biosci*. 2019;9:61. <https://doi.org/10.1186/s13578-019-0324-9>.
- Hartmann P, Chu H, Duan Y, Schnabl B. Gut microbiota in liver disease: too much is harmful, nothing at all is not helpful either. *Am J Physiol Gastrointest Liver Physiol*. 2019;316(5):G563–73. <https://doi.org/10.1152/ajpgi.00370.2018>.
- Tilg H, Zmora N, Adolph TE, Elinav E. The intestinal microbiota fuelling metabolic inflammation. *Nat Rev Immunol*. 2020;20(1):40–54. <https://doi.org/10.1038/s41577-019-0198-4>.
- Biagi E, Franceschi C, Rampelli S, Severgnini M, Ostan R, Turroni S, et al. Gut microbiota and extreme longevity. *Curr Biol*. 2016;26(11):1480–5. <https://doi.org/10.1016/j.cub.2016.04.016>.
- Fransen F, van Beek AA, Borghuis T, Aidy SE, Hugenholtz F, van der Gaast-de JC, et al. Aged gut microbiota contributes to systemical inflammaging after transfer to germ-free mice. *Front Immunol*. 2017;8:1385. <https://doi.org/10.3389/fimmu.2017.01385>.
- Binyamin D, Werbner N, Nuriel-Ohayon M, Uzan A, Mor H, Abbas A, et al. The aging mouse microbiome has obesogenic characteristics. *Genome Med*. 2020;12(1):87. <https://doi.org/10.1186/s13073-020-00784-9>.
- Backhed F, Manchester JK, Semenkovich CF, Gordon JI. Mechanisms underlying the resistance to diet-induced obesity in germ-free mice. *Proc Natl Acad Sci U S A*. 2007;104(3):979–84. <https://doi.org/10.1073/pnas.0605374104>.
- Parseus A, Sommer N, Sommer F, Caesar R, Molinaro A, Stahlman M, et al. Microbiota-induced obesity requires farnesoid X receptor. *Gut*. 2017;66(3):429–37. <https://doi.org/10.1136/gutjnl-2015-310283>.
- Thevaranjan N, Puchta A, Schulz C, Naidoo A, Szamosi JC, Verschoor CP, et al. Age-associated microbial dysbiosis promotes intestinal permeability, systemic inflammation, and macrophage dysfunction. *Cell Host Microbe*. 2017;21(4):455–66 e4. <https://doi.org/10.1016/j.chom.2017.03.002>.
- Kindt A, Liebisch G, Clavel T, Haller D, Hormannspurger G, Yoon H, et al. The gut microbiota promotes hepatic fatty acid desaturation and elongation in mice. *Nat Commun*. 2018;9(1):3760. <https://doi.org/10.1038/s41467-018-05767-4>.
- Velagapudi VR, Hezaveh R, Reigstad CS, Gopalacharyulu P, Yetukuri L, Islam S, et al. The gut microbiota modulates host energy and lipid metabolism in mice. *J Lipid Res*. 2010;51(5):1101–12. <https://doi.org/10.1194/jlr.M002774>.
- Sayin SI, Wahlstrom A, Felin J, Jantti S, Marschall HU, Bamberg K, et al. Gut microbiota regulates bile acid metabolism by reducing the levels of tauro-beta-muricholic acid, a naturally occurring FXR antagonist. *Cell Metab*. 2013;17(2):225–35. <https://doi.org/10.1016/j.cmet.2013.01.003>.
- Selwyn FP, Cheng SL, Bammler TK, Prasad B, Vrana M, Klaassen C, et al. Developmental regulation of drug-processing genes in livers of germ-free mice. *Toxicol Sci*. 2015;147(1):84–103. <https://doi.org/10.1093/toxsci/kfv110>.
- Ma J, Hong Y, Zheng N, Xie G, Lyu Y, Gu Y, et al. Gut microbiota remodeling reverses aging-associated inflammation and dysregulation of systemic bile acid homeostasis in mice sex-specifically. *Gut Microbes*. 2020;11(5):1450–74. <https://doi.org/10.1080/19490976.2020.1763770>.
- Smiraglia A, Lorito N, Serra M, Perra A, Morandi A, Kowalik MA. Sex difference in liver diseases: how preclinical models help to dissect the sex-related mechanisms sustaining NAFLD and hepatocellular carcinoma. *iScience*. 2023;26(12):108363. <https://doi.org/10.1016/j.isci.2023.108363>.
- Tsugawa H, Ishihara T, Ogasa K, Iwanami S, Hori A, Takahashi M, et al. A lipidome landscape of aging in mice. *Nat Aging*. 2024;4(5):709–26. <https://doi.org/10.1038/s43587-024-00610-6>.
- Dobin A, Davis CA, Schlesinger F, Drenkow J, Zaleski C, Jha S, et al. STAR: ultrafast universal RNA-seq aligner. *Bioinformatics*. 2013;29(1):15–21. <https://doi.org/10.1093/bioinformatics/bts635>.
- Robinson MD, McCarthy DJ, Smyth GK. edgeR: a bioconductor package for differential expression analysis of digital gene expression data. *Bioinformatics*. 2010;26(1):139–40. <https://doi.org/10.1093/bioinformatics/btp616>.
- Subramanian A, Tamayo P, Mootha VK, Mukherjee S, Ebert BL, Gillette MA, et al. Gene set enrichment analysis: a knowledge-based approach for interpreting genome-wide expression profiles. *Proc Natl Acad Sci U S A*. 2005;102(43):15545–50. <https://doi.org/10.1073/pnas.0506580102>.
- Zou Z, Ohta T, Oki S. ChIP-Atlas 3.0: a data-mining suite to explore chromosome architecture together with large-scale regulome data. *Nucleic Acids Res*. 2024;52(W1):W45–53. <https://doi.org/10.1093/nar/gkae358>.
- Srivastava A, Barth E, Ermolaeva MA, Guenther M, Frahm C, Marz M, et al. Tissue-specific gene expression changes are associated with aging in mice. *Genomics Proteomics Bioinformatics*. 2020;18(4):430–42. <https://doi.org/10.1016/j.gpb.2020.12.001>.
- Jonker MJ, Melis JP, Kuiper RV, van der Hoeven TV, Wackers PFK, Robinson J, et al. Life spanning murine gene expression profiles in relation to chronological and pathological aging in multiple organs. *Aging Cell*. 2013;12(5):901–9. <https://doi.org/10.1111/acer.12118>.
- Yoshimoto S, Loo TM, Atarashi K, Kanda H, Sato S, Oyadomari S, et al. Obesity-induced gut microbial metabolite promotes liver cancer through senescence secretome. *Nature*. 2013;499(7456):97–101. <https://doi.org/10.1038/nature12347>.
- Lefebvre P, Staels B. Hepatic sexual dimorphism - implications for non-alcoholic fatty liver disease. *Nat Rev Endocrinol*. 2021;17(11):662–70. <https://doi.org/10.1038/s41574-021-00538-6>.
- Burra P, Zanetto A, Schnabl B, Reiberger T, Montano-Loza AJ, Asselta R, et al. Hepatic immune regulation and sex disparities. *Nat Rev Gastroenterol Hepatol*. 2024;21(12):869–84. <https://doi.org/10.1038/s41575-024-00974-5>.
- Holloway MG, Miles GD, Dombkowski AA, Waxman DJ. Liver-specific hepatocyte nuclear factor-4alpha deficiency: greater impact on gene expression in male than in female mouse liver. *Mol Endocrinol*. 2008;22(5):1274–86. <https://doi.org/10.1210/me.2007-0564>.
- Li Z, Tuteja G, Schug J, Kaestner KH. Foxa1 and Foxa2 are essential for sexual dimorphism in liver cancer. *Cell*. 2012;148(1–2):72–83. <https://doi.org/10.1016/j.cell.2011.11.026>.
- Dubois V, Eeckhoutte J, Lefebvre P, Staels B. Distinct but complementary contributions of PPAR isotypes to energy homeostasis. *J Clin Invest*. 2017;127(4):1202–14. <https://doi.org/10.1172/JCI88894>.
- Pastore N, Brady OA, Diab HI, Martina JA, Sun L, Huynh T, et al. TFEB and TFE3 cooperate in the regulation of the innate immune response in activated macrophages. *Autophagy*. 2016;12(8):1240–58. <https://doi.org/10.1080/15548627.2016.1179405>.
- Liu T, Zhang L, Joo D, Sun SC. NF-kappaB signaling in inflammation. *Signal Transduct Target Ther*. 2017;2:17023-. <https://doi.org/10.1038/sigtr.ans.2017.23>.
- Runge-Morris M, Kocarek TA, Falany CN. Regulation of the cytosolic sulfotransferases by nuclear receptors. *Drug Metab Rev*. 2013;45(1):15–33. <https://doi.org/10.3109/03602532.2012.748794>.

38. Sanchez LD, Pontini L, Marinozzi M, Sanchez-Aranguren LC, Reis A, Dias IHK. Cholesterol and oxysterol sulfates: pathophysiological roles and analytical challenges. *Br J Pharmacol*. 2021;178(16):3327–41. <https://doi.org/10.1111/bph.15227>.
39. Xu R, Antwi Boasiako P, Mao C. Alkaline ceramidase family: the first two decades. *Cell Signal*. 2021;78:109860. <https://doi.org/10.1016/j.cellsig.2020.109860>.
40. Valentine WJ, Yanagida K, Kawana H, Kono N, Noda NN, Aoki J, et al. Update and nomenclature proposal for mammalian lysophospholipid acyltransferases, which create membrane phospholipid diversity. *J Biol Chem*. 2022;298(1):101470. <https://doi.org/10.1016/j.jbc.2021.101470>.
41. Hishikawa D, Yanagida K, Nagata K, Kanatani A, Iizuka Y, Hamano F, et al. Hepatic levels of DHA-containing phospholipids instruct SREBP1-mediated synthesis and systemic delivery of polyunsaturated fatty acids. *iScience*. 2020;23(9):101495. <https://doi.org/10.1016/j.isci.2020.101495>.
42. Jacobs A, Warda AS, Verbeek J, Cassiman D, Spincemaille P. An overview of mouse models of nonalcoholic steatohepatitis: from past to present. *Curr Protoc Mouse Biol*. 2016;6(2):185–200. <https://doi.org/10.1002/cpmo.3>.
43. Hammerich L, Tacke F. Hepatic inflammatory responses in liver fibrosis. *Nat Rev Gastroenterol Hepatol*. 2023;20(10):633–46. <https://doi.org/10.1038/s41575-023-00807-x>.
44. Kim HY, Sakane S, Eguileor A, Carvalho Gontijo Weber R, Lee W, Liu X, et al. The origin and fate of liver myofibroblasts. *Cell Mol Gastroenterol Hepatol*. 2024;17(1):93–106. <https://doi.org/10.1016/j.jcmgh.2023.09.008>.
45. He X, Sun Z, Sun J, Chen Y, Luo Y, Wang Z, et al. Single-cell transcriptomics reveal the microenvironment landscape of perfluorooctane sulfonate-induced liver injury in female mice. *Sci Total Environ*. 2024;940:173562. <https://doi.org/10.1016/j.scitotenv.2024.173562>.
46. Wei Y, Zeng B, Chen J, Cui G, Lu C, Wu W, et al. Enterogenous bacterial glycolipids are required for the generation of natural killer T cells mediated liver injury. *Sci Rep*. 2016;6:36365. <https://doi.org/10.1038/srep36365>.
47. Tosello-Trampont AC, Landes SG, Nguyen V, Novobrantseva TI, Hahn YS. Kupffer cells trigger nonalcoholic steatohepatitis development in diet-induced mouse model through tumor necrosis factor- α production. *J Biol Chem*. 2012;287(48):40161–72. <https://doi.org/10.1074/jbc.M112.417014>.
48. Li H, Xia N. The multifaceted roles of B lymphocytes in metabolic dysfunction-associated steatotic liver disease. *Front Immunol*. 2024;15:1447391. <https://doi.org/10.3389/fimmu.2024.1447391>.
49. Iyer S, Upadhyay PK, Majumdar SS, Nagarajan P. Animal models correlating immune cells for the development of NAFLD/NASH. *J Clin Exp Hepatol*. 2015;5(3):239–45. <https://doi.org/10.1016/j.jceh.2015.06.004>.
50. Mao T, Yang R, Luo Y, He K. Crucial role of T cells in NAFLD-related disease: a review and prospect. *Front Endocrinol (Lausanne)*. 2022;13:1051076. <https://doi.org/10.3389/fendo.2022.1051076>.
51. Ohashi T, Kato M, Yamasaki A, Kuwano A, Suzuki H, Kohjima M, et al. Effects of high fructose intake on liver injury progression in high fat diet induced fatty liver disease in ovariectomized female mice. *Food Chem Toxicol*. 2018;118:190–7. <https://doi.org/10.1016/j.fct.2018.05.006>.
52. Martin-Murphy BV, You Q, Wang H, De La Houssaye BA, Reilly TP, Friedman JE, et al. Mice lacking natural killer T cells are more susceptible to metabolic alterations following high fat diet feeding. *PLoS One*. 2014;9(1):e80949. <https://doi.org/10.1371/journal.pone.0080949>.
53. Mocchegiani E, Malavolta M. NK and NKT cell functions in immunosenescence. *Aging Cell*. 2004;3(4):177–84. <https://doi.org/10.1111/j.1474-9728.2004.00107.x>.
54. Park SH, Wiwi CA, Waxman DJ. Signalling cross-talk between hepatocyte nuclear factor 4 α and growth-hormone-activated STAT5b. *Biochem J*. 2006;397(1):159–68. <https://doi.org/10.1042/BJ20060332>.
55. Holloway MG, Laz EV, Waxman DJ. Codependence of growth hormone-responsive, sexually dimorphic hepatic gene expression on signal transducer and activator of transcription 5b and hepatic nuclear factor 4 α . *Mol Endocrinol*. 2006;20(3):647–60. <https://doi.org/10.1210/me.2005-0328>.
56. Clodfelter KH, Miles GD, Wauthier V, Holloway MG, Zhang X, Hodor P, et al. Role of STAT5a in regulation of sex-specific gene expression in female but not male mouse liver revealed by microarray analysis. *Physiol Genomics*. 2007;31(1):63–74. <https://doi.org/10.1152/physiolgenomics.00055.2007>.
57. Zhang Y, Laz EV, Waxman DJ. Dynamic, sex-differential STAT5 and BCL6 binding to sex-biased, growth hormone-regulated genes in adult mouse liver. *Mol Cell Biol*. 2012;32(4):880–96. <https://doi.org/10.1128/MCB.06312-11>.
58. Conforto TL, Zhang Y, Sherman J, Waxman DJ. Impact of CUX2 on the female mouse liver transcriptome: activation of female-biased genes and repression of male-biased genes. *Mol Cell Biol*. 2012;32(22):4611–27. <https://doi.org/10.1128/MCB.00886-12>.
59. Waxman DJ, O'Connor C. Growth hormone regulation of sex-dependent liver gene expression. *Mol Endocrinol*. 2006;20(11):2613–29. <https://doi.org/10.1210/me.2006-0007>.
60. Nikkanen J, Leong YA, Krause WC, Dermadi D, Maschek JA, Van Ry T, et al. An evolutionary trade-off between host immunity and metabolism drives fatty liver in male mice. *Science*. 2022;378(6617):290–5. <https://doi.org/10.1126/science.abn9886>.
61. Waxman DJ, Holloway MG. Sex differences in the expression of hepatic drug metabolizing enzymes. *Mol Pharmacol*. 2009;76(2):215–28. <https://doi.org/10.1124/mol.109.056705>.
62. Penn DJ, Zala SM, Luzynski KC. Regulation of sexually dimorphic expression of major urinary proteins. *Front Physiol*. 2022;13:822073. <https://doi.org/10.3389/fphys.2022.822073>.
63. Lu M, Flanagan JU, Langley RJ, Hay MP, Perry JK. Targeting growth hormone function: strategies and therapeutic applications. *Signal Transduct Target Ther*. 2019;4:3. <https://doi.org/10.1038/s41392-019-0036-y>.
64. Weger BD, Gobet C, Yeung J, Martin E, Jimenez S, Betrisey B, et al. The mouse microbiome is required for sex-specific diurnal rhythms of gene expression and metabolism. *Cell Metab*. 2019;29(2):362–82 e8. <https://doi.org/10.1016/j.cmet.2018.09.023>.
65. Milletta MC, Petkovic V, Eble A, Ammann RA, Fluck CE, Mullis PE. Butyrate increases intracellular calcium levels and enhances growth hormone release from rat anterior pituitary cells via the G-protein-coupled receptors GPR41 and 43. *PLoS One*. 2014;9(10):e107388. <https://doi.org/10.1371/journal.pone.0107388>.
66. Fuller KNZ, McCoin CS, Von Schulze AT, Houchen CJ, Choi MA, Thyfault JP. Estradiol treatment or modest exercise improves hepatic health and mitochondrial outcomes in female mice following ovariectomy. *Am J Physiol Endocrinol Metab*. 2021;320(6):E1020–31. <https://doi.org/10.1152/ajpendo.00013.2021>.
67. Khaksari M, Pourali M, Rezaei Talabon S, Gholizadeh Navashenaq J, Bashiri H, Amiresmaili S. Protective effects of 17- β -estradiol on liver injury: the role of TLR4 signaling pathway and inflammatory response. *Cytokine*. 2024;181:156686. <https://doi.org/10.1016/j.cyto.2024.156686>.
68. Alnouti Y, Klaassen CD. Mechanisms of gender-specific regulation of mouse sulfotransferases (Sults). *Xenobiotica*. 2011;41(3):187–97. <https://doi.org/10.3109/00498254.2010.535923>.
69. Xu D, Ma R, Ju Y, Song X, Niu B, Hong W, et al. Cholesterol sulfate alleviates ulcerative colitis by promoting cholesterol biosynthesis in colonic epithelial cells. *Nat Commun*. 2022;13(1):4428. <https://doi.org/10.1038/s41467-022-32158-7>.
70. Wang F, Beck-Garcia K, Zorzin C, Schamel WW, Davis MM. Inhibition of T cell receptor signaling by cholesterol sulfate, a naturally occurring derivative of membrane cholesterol. *Nat Immunol*. 2016;17(7):844–50. <https://doi.org/10.1038/ni.3462>.
71. Shimizu C, Fuda H, Yanai H, Strott CA. Conservation of the hydroxysteroid sulfotransferase SULT2B1 gene structure in the mouse: pre- and postnatal expression, kinetic analysis of isoforms, and comparison with prototypical SULT2A1. *Endocrinology*. 2003;144(4):1186–93. <https://doi.org/10.1210/en.2002-221011>.
72. Omae F, Miyazaki M, Enomoto A, Suzuki M, Suzuki Y, Suzuki A. DES2 protein is responsible for phytoceramide biosynthesis in the mouse small intestine. *Biochem J*. 2004;379(Pt 3):687–95. <https://doi.org/10.1042/BJ20031425>.
73. Ota A, Morita H, Naganuma T, Miyamoto M, Jojima K, Nojiri K, et al. Bifunctional DEGS2 has higher hydroxylase activity toward substrates with very-long-chain fatty acids in the production of phytosphingosine ceramides. *J Biol Chem*. 2023;299(4):104603. <https://doi.org/10.1016/j.jbc.2023.104603>.
74. Wang K, Li C, Lin X, Sun H, Xu R, Li Q, et al. Targeting alkaline ceramidase 3 alleviates the severity of nonalcoholic steatohepatitis by reducing oxidative stress. *Cell Death Dis*. 2020;11(1):28. <https://doi.org/10.1038/s41419-019-2214-9>.
75. Murakami I, Wakasa Y, Yamashita S, Kurihara T, Zama K, Kobayashi N, et al. Phytoceramide and sphingoid bases derived from brewer's yeast

- Saccharomyces pastorianus* activate peroxisome proliferator-activated receptors. *Lipids Health Dis.* 2011;10:150. <https://doi.org/10.1186/1476-511X-10-150>.
76. Maricic I, Girardi E, Zajonc DM, Kumar V. Recognition of lysophosphatidylcholine by type II NKT cells and protection from an inflammatory liver disease. *J Immunol.* 2014;193(9):4580–9. <https://doi.org/10.4049/jimmunol.1400699>.
 77. Yan JJ, Jung JS, Lee JE, Lee J, Huh SO, Kim HS, et al. Therapeutic effects of lysophosphatidylcholine in experimental sepsis. *Nat Med.* 2004;10(2):161–7. <https://doi.org/10.1038/nm989>.
 78. Hung ND, Kim MR, Sok DE. 2-Polyunsaturated acyl lysophosphatidylethanolamine attenuates inflammatory response in zymosan A-induced peritonitis in mice. *Lipids.* 2011;46(10):893–906. <https://doi.org/10.1007/s11745-011-3589-2>.
 79. Park SJ, Im DS. 2-Arachidonyl-lysophosphatidylethanolamine induces anti-inflammatory effects on macrophages and in carrageenan-induced paw edema. *Int J Mol Sci.* 2021;22(9):4865. <https://doi.org/10.3390/ijms22094865>.
 80. Liu P, Zhu W, Chen C, Yan B, Zhu L, Chen X, et al. The mechanisms of lysophosphatidylcholine in the development of diseases. *Life Sci.* 2020;247:117443. <https://doi.org/10.1016/j.lfs.2020.117443>.
 81. Tan ST, Ramesh T, Toh XR, Nguyen LN. Emerging roles of lysophospholipids in health and disease. *Prog Lipid Res.* 2020;80:101068. <https://doi.org/10.1016/j.plipres.2020.101068>.
 82. Ishihara T, Yoshida M, Arita M. Omega-3 fatty acid-derived mediators that control inflammation and tissue homeostasis. *Int Immunol.* 2019;31(9):559–67. <https://doi.org/10.1093/intimm/dxz001>.
 83. Papsdorf K, Brunet A. Linking lipid metabolism to chromatin regulation in aging. *Trends Cell Biol.* 2019;29(2):97–116. <https://doi.org/10.1016/j.tcb.2018.09.004>.
 84. Rauluseviciute I, Riudavets-Puig R, Blanc-Mathieu R, Castro-Mondragon JA, Ferenc K, Kumar V, et al. JASPAR 2024: 20th anniversary of the open-access database of transcription factor binding profiles. *Nucleic Acids Res.* 2024;52(D1):D174–82. <https://doi.org/10.1093/nar/gkad1059>.
 85. Montoliu I, Scherer M, Beguelin F, DaSilva L, Mari D, Salvioli S, et al. Serum profiling of healthy aging identifies phospho- and sphingolipid species as markers of human longevity. *Aging (Albany NY).* 2014;6(1):9–25. <https://doi.org/10.18632/aging.100630>.
 86. Yu Z, Zhai G, Singmann P, He Y, Xu T, Prehn C, et al. Human serum metabolic profiles are age dependent. *Aging Cell.* 2012;11(6):960–7. <https://doi.org/10.1111/j.1474-9726.2012.00865.x>.
 87. Gorden DL, Myers DS, Ivanova PT, Fahy E, Maurya MR, Gupta S, et al. Biomarkers of NAFLD progression: a lipidomics approach to an epidemic. *J Lipid Res.* 2015;56(3):722–36. <https://doi.org/10.1194/jlr.P056002>.

Publisher's Note

Springer Nature remains neutral with regard to jurisdictional claims in published maps and institutional affiliations.